COMPRESSION AND TENSION IN MODEL VENUS HIGHLANDS PARTLY DECOUPLED FROM MANTLE FLOW. W. Roger Buck[1] and James W. Head[2], [1]Lamont-Doherty Earth Observatory of Columbia University, Palisades, NY 10964 USA(buck@ldeo.columbia.edu), [2]Department of Earth, Environmental and Planetary Sciences, Brown University, Providence, RI 02912 USA. (James_Head@brown.edu)

Introduction: Venus, the most Earth-like of the terrestrial planets in size, density, and position in the Solar System, has long been an attractive exploration target to obtain geodynamic and atmospheric evolution data that might help explain its profoundly un-Earth like current atmosphere (dominantly CO_2; P_{atm} ~93 bars; 737 K surface temperature). At issue has been the nature of the global surface geology (old, young, or an Earth-like ratio of both?), its tectonic style (Earth-like plate tectonics?), the major modes of lithospheric heat transfer (conduction, advection, plate recycling?) [1], and the significance of the extremely high surface temperatures in influencing tectonic style and volcanism [2].

Early missions (Venera 15-16) provided regional context for the presence of rifted equatorial rises and high-latitude highlands ringed by folded mountain belts seen in Earth-based radar, leading to hypotheses that Venus might be characterized by equatorial plate tectonic crustal spreading and northern convergent subduction zones. In contrast, global Magellan data clearly demonstrated that Venus was currently a one-plate planet, losing heat largely by conduction, and that it may have undergone global-scale tectonic and volcanic resurfacing less than a billion years ago [3].

What, then, are the dominant geodynamic styles on recent Venus [4]? Global geological mapping [5] showed that the oldest terrains were highly deformed, thick crust, tessera highlands (large-scale folding, shear and extension), followed by extensive global volcanic plains (deformation belts interpreted to represent both compression and tension), and a global network of young interconnected rift zones. These observations led to several decades of debate about their geodynamic significance: Did the tessera highlands terrain represent upwelling or downwelling [6-7]? What was the influence of the high surface temperatures on lithospheric thermal structure and deformation, and deeper crustal and mantle rheological properties? What was the origin and timing of the ubiquitous parallel graben ('ribbon terrain') in the tessera and its relationship to other tessera structure [8-10]? Community consensus on these questions has not yet been reached, and a broad-scale paradigm for the interpretation of compressional and extensional features in the Venus highlands has remained elusive.

In this analysis, we revisit and update earlier assessments of the role of elevated surface temperatures on the temperature-dependent rheology of the lower crust, and its relationship to underlying mantle convection patterns and rates [11-14]; we then use this paradigm to revisit some of these key questions.

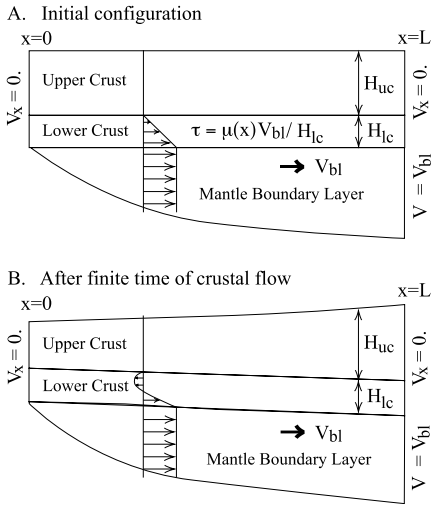

Figure 1. (A) shows the initial set up for analytic and numerical model calculations of lower crustal flow driven by horizontal motion of a mantle boundary layer. The lateral position x=0 is a region of mantle divergence and x=L is a place of mantle convergence. (B) Shows the way thickening of the crust over the zone of convergence can drive flow opposite to the mantle motion.

Model Description: The model setup and the evolution of crustal thickness follows an earlier work [15], updating the calculation of tectonic forces reported there. We assume that the crust of Venus can be approximated by 2 layers with an upper crust that is elastic and brittle and a lower crustal layer of thickness H_L that deforms primarily by viscous flow as shown in Figure 1. The mantle below the crust is convecting with a horizontal cell length L and we approximate the top of the mantle as having a uniform horizontal velocity $V_{BL.}$ Assuming that $H_{LC} \ll L$ we can then use the thin channel approximation to calculate the horizontal velocity variation within the layer.

Local isostatic topography due to crustal thickness variations is computed for a crustal density of 2900 kg-m^{-3} and a mantle density of 3300 kg-m^{-3}. The tectonic force in the upper crust is taken to be the integrated basal stress from x=0 to x=L.

An analytic version of the model for a lower crust with constant properties is used to show that as the crust thickens, the stress in the upper crust over a zone of convergence can switch from compression to extension, similar to relationships seen in some tessera [16]. For a constant thickness of the lower crust, extension of highlands begins when the model topographic relief reaches a third of the maximum possible relief.

A simple numerical version of the model is formulated with lateral variations in the temperature and, and thus the viscosity of the lower crust. The viscosity of the lower crust is taken to have a Newtonian viscosity μ that depends on exponentially on inverse absolute temperature. The thickness of the lower crust is kept constant at 10 km and a uniform viscosity is set by the temperature at the base of the crust. The temperature there is taken to be linearly related to the heat flow coming out of the mantle boundary layer assuming that the mantle and the crust have the same thermal conductivity. The temperature at the surface of the crust is 723K. The upper crustal thickness is initially 20 km, but as the lower crust is thickened or thinned, the changes are taken to occur in the upper crust (i.e. for simplicity the lower crust has a constant thickness). The lower crustal viscosity is set to have a reference value at a temperature of 1000K and the temperature of the lower crust does not evolve with time.

The mantle heat flow with distance from a zone of mantle divergence is computed from a half-space cooling model analogous to the way oceanic plate cooling is often treated. The temperature difference across the mantle boundary layer is taken to be 500K and the thermal diffusivity is 10^{-6} m-s^{-2}.

Numerical Results: For the illustrative model cases shown in Figure 2, all the model parameters are the same except that the velocity of the mantle differs by a factor of 2. The reference viscosity here was set to $3x10^{17}$ Pas to give a reasonable range of topography though this is well below the value predicted for dry diabase [17]. The numerical model results are very sensitive to the rate of lateral mantle flow because the crustal viscosity is strongly temperature dependent and the temperature in the model lower crust depends on the rate of flow of the mantle. The slower mantle velocities can lead to a slower increase of relief, but the ultimate relief is always larger for the slow velocities.

The tectonic force in the upper crust above the zone of mantle convergence is always compressional to begin with and eventually transitions to extensional. The magnitude of the tectonic forces can reach levels that could drive rifting of moderately thick upper crust. For the 10 cm/yr case in Figure 2 (B) after 50 Myrs the extensional tectonic force is nearly $4x10^{11}$ N/m and this is sufficient to drive extensional faulting through a nearly 10 km thick brittle layer based on standard assumptions and rock friction [18].

These preliminary results point to rates of crustal thickening and thinning, and predicted accompanying crustal thicknesses, topographic evolution, and sign and sequence of faulting that can be compared to the array of tectonic and topographic features observed on Venus, and their stratigraphic relations [5, 19]. The thickening of crust under highlands including rifted highlands is consistent with geoid elevation relations for those areas [20].

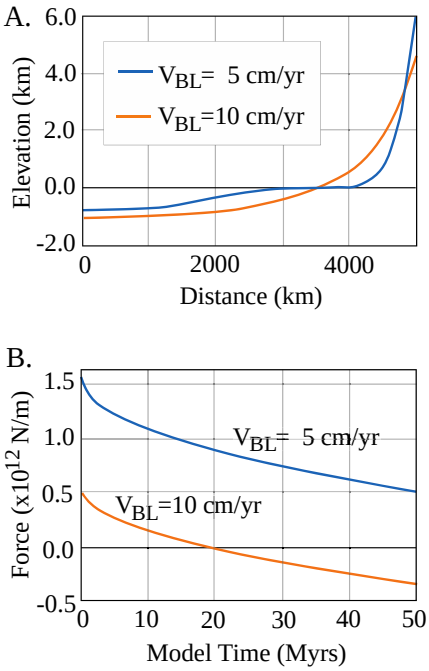

Figure 2. Results of numerical model calculations for two cases that differ only in the mantle boundary layer velocity. (A) shows topographic relief after 50 myrs of model time. (B) shows evolution of tectonic force in the upper crust at the point of mantle convergence (x=L). For the case with V_{bl} = 10 cm/yr the force changes from compressional (positive) to extensional (negative).

References: 1. Solomon, S.C. & Head, J.W., 1982. *JGR 87*, 9236. 2. Solomon, S.C., Bullock, M.A. & Grinspoon, D.H., 1999. *Science 286*, 87. 3. Head, J.W., 2014. *Geology 42*, 95. 4. Smrekar, S.E., Davaille, A. & Sotin, C., 2018. *Space Science Reviews*, *214*, 1. 5. Ivanov, M.A. & Head, J.W., 2011. *Planetary and Space Science 59*,1559. 6. Hansen, V.L., Phillips, R.J., Willis, J.J. & Ghent, R.R., 2000. *JGR Planets 105*, 4135. 7. Bindschadler, D.L. & Head, J.W., 1991. *JGR 96*, 5889. 8. Hansen, V.L., 2006. *JGR Planets 111*, E11. 9. Hansen, V.L. & Willis, J.J., 1998. *Icarus 132*, 321. 10. Hanmer, S., 2020. *Earth-Science Reviews*, *201*, 103077. 11. Smerkar S.E. & Phillips, R.J, 1988, *GRL 15*, 693. 12. Grimm, R.E & Solomon, S.C, 1988, *JGR 93*, 11,911. 13. Bindschadler, D.L. & Parmentier, E.M. 1990, *JGR 95*, 20,329. 14. Kiefer, W.S. & Hagar, B.H., 1991, *JGR 96*, 20,967. 15. Buck, W.R., 1992, *GRL 19*, 2011. 16. Ivanov, M.A. & Head, J.W., 1996. *JGR Planets 101*, 14861. 17. Mackwell, S.J., Zimmermann, M.E. & Kohlstedt, D.L., 1998, *JGR 103*, 975. 18. Turcotte, D.L & Schubert, G., 2014, *Geodynamics*, 828p. 19. Byrne, P.K. et al., 2021, *PNAS 118*, 26., 20. James, P.B., Zuber, M.T. & Phillips, R.J., 2013, *JGR 118*, 859.